บทความวิจัย

การศึกษาสารเชิงซ้อนของโลหะกับกรดลิวอิส Pt(PB) และ Pt(PAl) สำหรับการสลายพันธะของไฮโดรเจนและการเติมไฮโดรเจนแก่เอทิลีนด้วยวิธีทางทฤษฎีฟังก์ชันนัลความหนาแน่น

มูฮัมหมัด ดซูลฟามี รามาดฮัน[1] และพนิดา สุรวัฒนาวงศ์[1, 2*]

[1]ภาควิชาเคมีและศูนย์ความเป็นเลิศด้านนวัตกรรมทางเคมี คณะวิทยาศาสตร์ มหาวิทยาลัยมหิดล กรุงเทพมหานคร 10400 ประเทศไทย

[2]หน่วยวิจัยพลังงานยั่งยืนและวัสดุสีเขียว มหาวิทยาลัยมหิดล นครปฐม 73170 ประเทศไทย

**Email: panida.sur@mahidol.ac.th*

รับบทความ: 27 เมษายน 2564 แก้ไขบทความ: 23 พฤษภาคม 2564 ยอมรับตีพิมพ์: 23 พฤษภาคม 2564

บทคัดย่อ

โลหะทรานซิชันหมู่ 10 (M = Pt, Ni) สามารถทำงานร่วมกับกรดลิวอิส (Z = B, Al) เพื่อสลายพันธะของไฮโดรเจนได้ การศึกษาด้วยวิธีทางทฤษฎีฟังก์ชันนัลความหนาแน่นแสดงให้เห็นว่า สารเชิงซ้อน **1Pt(PAl)** ซึ่งประกอบด้วยลิแกนด์ $Mes_2PC(=CHPh)Al^tBu_2$ (**PAl**) เกาะกับโลหะแพลตตินัมสามารถทำงานร่วมกันในการสลายพันธะของไฮโดรเจนผ่านทรานซิชันสเตท **TS12_PtAl** ซึ่งมีโครงสร้างเป็นแบบตัวที ด้วยพลังงานกระตุ้นอิสระเท่ากับ 31.6 kcal/mol สอดคล้องกับผลการทดลองที่พบว่า สารเชิงซ้อนนี้สามารถสลายพันธะของไฮโดรเจนได้ที่อุณหภูมิ 80 °C จากนั้นเราได้แทนที่อลูมิเนียมซึ่งทำหน้าที่ของกรดลิวอิสด้วยโบรอน โดย **1Pt(PB)** ต่างจาก **1Pt(PAl)** ตรงที่ไม่พบอันตรกิริยาระหว่าง Pt—B (3.154 Å) **1Pt(PB)** จึงมีความไวต่อการสลายพันธะของไฮโดรเจนมากขึ้น ด้วยพลังงานกระตุ้นอิสระลดลงเป็น 21.8 kcal/mol เมื่อมีการใช้โลหะนิกเกิลซึ่งมีความเป็นอิเล็กโตรโพสิทีฟแทนที่แพลตตินัมสำหรับ **1Ni(PB)** แทนที่ **1Pt(PB)** พบว่า มีความไวต่อปฏิกิริยาการสลายพันธะของไฮโดรเจนมากขึ้นอีก ด้วยพลังงานกระตุ้นอิสระเพียง 9.7 kcal/mol ในขณะที่ทรานซิชันสเตท **TS12_PtB** ของสารเชิงซ้อนแพลตตินัมมีโครงสร้างแบบตัวที ทรานซิชันสเตท **TS12_NiB** ของสารเชิงซ้อนนิกเกิลมีโครงสร้างใกล้กับเตตระฮีดรอน เราได้ทำการวิเคราะห์พลังงานกระตุ้นอิสระด้วยการแยกพิจารณาเป็นส่วนของพลังงานอันตรกิริยาระหว่างสารเชิงซ้อนกับไฮโดรเจน และส่วนของพลังงานที่ใช้การปรับโครงสร้างจากสารเชิงซ้อนในรูปอิสระไปเป็นโครงสร้างสารเชิงซ้อนในรูปที่มีไฮโดรเจนกำลังแตกพันธะที่ทรานซิชันสเตท สารผลิตภัณฑ์ที่ได้จากการสลายพันธะของไฮโดรเจนสามารถเติมไฮโดรเจนแก่เอทิลีนได้ โดยขั้นกำหนดปฏิกิริยา คือ ขั้นตอนที่มีการถ่ายโอนไฮโดรเจนครั้งที่หนึ่งจาก **2M(PZ)** ไปยังคาร์บอนของเอทิลีนผ่านทรานซิชันสเตท **TS23_MZ** ในขั้นการเติมไฮโดรเจนแก่เอทิลีนนี้ **1Ni(PB)** อาศัยพลังงานกระตุ้นอิสระเท่ากับ 26.3 kcal/mol ซึ่งเป็นค่าที่ต่ำสุดเทียบกับสารเชิงซ้อนโลหะอื่นในการศึกษานี้ แผนภูมิพลังงานจากการศึกษาด้วยวิธีทางคอมพิวเตอร์ในงานวิจัยนี้ใช้เป็นแนวทางการพัฒนาสารเชิงซ้อนของโลหะกับกรดลิวอิสที่มีความไวต่อปฏิกิริยาได้ต่อไป

คำสำคัญ: การสลายพันธะของไฮโดรเจน การเติมไฮโดรเจนแก่เอทิลีน ทฤษฎีฟังก์ชันนัลความหนาแน่น แพลตตินัม นิกเกิล กรดลิวอิส

อ้างอิงบทความนี้

มูฮัมหมัด ดซูลฟามี รามาดฮัน และพนิดา สุรวัฒนาวงศ์. (2564). การศึกษาสารเชิงซ้อนของโลหะกับกรดลิวอิส Pt(PB) และ Pt(PAl) สำหรับการสลายพันธะของไฮโดรเจนและการเติมไฮโดรเจนแก่เอทิลีนด้วยวิธีทางทฤษฎีฟังก์ชันนัลความหนาแน่น. **วารสารวิทยาศาสตร์และวิทยาศาสตร์ศึกษา**, 4(1), 11-21.

Research Article

Density functional study of metal Lewis acid complexes Pt(PB) and Pt(PAl) for H_2 activation and ethylene hydrogenation

Muhammad Dzulfahmi Ramadhan[1] **and Panida Surawatanawong**[1,2*]

[1]*Department of Chemistry and Center of Excellence for Innovation in Chemistry, Faculty of Science, Mahidol University, Bangkok 10400, Thailand*

[2]*Center of Sustainable Energy and Green Materials, Mahidol University, Salaya, Nakhon Pathom 73170, Thailand*

**Email: panida.sur@mahidol.ac.th*

Received <27 April 2021>; Revised <23 May 2021>; Accepted <23 May 2021>

Abstract

The transition metal group 10 (M = Pt, Ni) can work cooperatively with the Lewis acid (Z = B, Al) towards heterolytic H_2 activation. Our density functional study showed that **1Pt(PAl)**, the $Mes_2PC(=CHPh)Al^tBu_2$ (**PAl**) ligand in combination with platinum metal, enables cooperative dihydrogen activation via T-shaped transition state **TS12_PtAl** (31.6 kcal/mol), which is in accordance with the experimentally observed hydrogen activation at 80 °C. We then explored the possibility of using boron instead of aluminum Lewis acid. Unlike **1Pt(PAl)**, **1Pt(PB)** has no interaction between Pt—B (3.154 Å). This allows more facile activation of dihydrogen substrate, which leads to a lower energy barrier of 21.8 kcal/mol for **1Pt(PB)**. With the use of electropositive Ni in place of Pt, **1Ni(PB)** exhibited even higher reactivity towards H_2 with energy barrier of 9.7 kcal/mol. While the Pt complexes proceeded with the T-shape geometries in the formation of **TS12_PtB,** nickel complex bears the tetrahedral-like transition state, **TS12_NiB**. The distortion-interaction analysis was performed to evaluate the contribution that affects the height of energy barrier. Furthermore, the H_2 activation product was used to perform ethylene hydrogenation. The rate determining step was achieved through the first transfer of terminal hydrogen from **2M(PZ)** to the carbon of ethylene via transition state **TS23_MZ**. The energy required to proceed ethylene hydrogenation by **1Ni(PB)** was found to be most favorable among all metal complexes (26.3 kcal/mol). The energetic profile from this computational study can be used as a guide for potential reactivity of metal Lewis acid complexes.

Keywords: H_2 activation, ethylene hydrogenation, density functional theory, platinum, nickel, Lewis acid

Cite this article:

Ramadhan, M.D. and Surawatanawong, P. (2021). Density functional study of metal Lewis acid complexes Pt(PB) and Pt(PAl) for H_2 activation and ethylene hydrogenation. **Journal of Science and Science Education**, 4(1), 11-21.

Introduction

The H_2 bond cleavage has been a crucial step in the transformation of dihydrogen for the application in H_2 fuel cell energy storage, hydrogenation and dehydrogenation processes (Karunananda & Mankad, 2017; Khusnutdinova & Milstein, 2015). The H_2 activation can proceed through two possible pathways: (i) homolytic cleavage involving electron donation from σ-orbital of H_2 to an empty d-orbital of transition metal and the back electron-donation from a filled d-orbital of metal to σ^*-orbital of H_2 (Figure 1a) and (ii) heterolytic cleavage with the assistance of Lewis acid and/or base. While the H_2 activation by transition metal-free frustrated Lewis pairs (FLPs) (Holschumacher, Bannenberg, Hrib, Jones, & Tamm, 2008; Rokob & Pápai, 2013; Skara, De Vleeschouwer, Geerlings, De Proft, & Pinter, 2017; Spies et al., 2007; Welch, Juan, Masuda, & Stephan, 2006; Welch & Stephan, 2007) (Figure 1b) and by cooperative metal-Lewis base (M-LB) (Figure 1c) have been widely studied (Morris, 2015; Noyori, Yamakawa, & Hashiguchi, 2001), the H_2 activation by metal-Lewis acid (M-LA) complexes still remains a challenge (Tsoureas, Kuo, Haddow, & Owen, 2011; Zeng & Sakaki, 2013) (Figure 1d).

The heterolytic H-H bond cleavage by transition metal with the assistance of Lewis acid is achieved by electron donation from σ_{HH} to unoccupied *p*-orbital of Lewis acid, and the back electron-donation from d-orbital of metal to σ^*_{HH} orbital (Karunananda & Mankad, 2017). In addition to H_2 activation, the Lewis acidic ligand can assist the electron-rich transition metal for further catalytic hydrogenation (Devillard et al., 2016; Karunananda & Mankad, 2017; Zeng & Sakaki, 2013).

In 2011, Appelt and co-workers reported that $Mes_2PC(=CHPh)Al^tBu_2$ (**PAl**), the geminal frustrated Lewis pair, can undergo CO_2 addition at room temperature but cannot activate H_2 under ambient condition (Appelt et al., 2011). In 2016, Bourissou and co-workers reported that Pt supported by **PAl** as a ligand, $Pt(PPh_3)(Mes_2PC(=CHPh)Al^tBu_2)$, **1Pt(PAl)**, can proceed to CO_2 addition under ambient condition and can also enable the activation of H_2 at 80 °C (Devillard et al., 2016). The introduction of transition metal group 10 in cooperative with aluminum Lewis acid enhances the reactivity towards H_2.

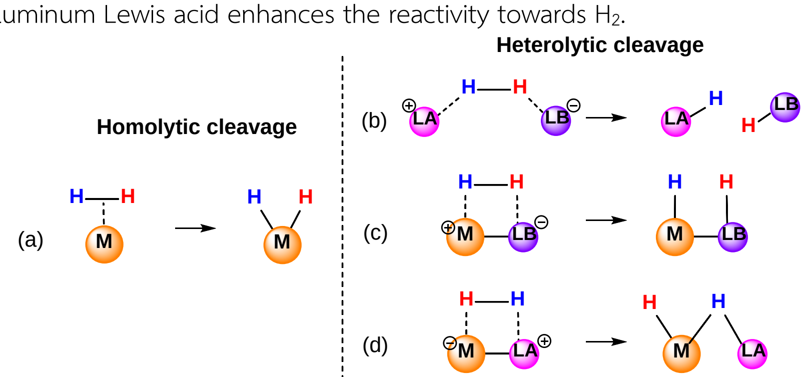

Figure 1. Catalytic H_2 activation: (a) single-site transition metal (M), (b) frustrated Lewis pair (LA-LB), (c) cooperative metal-Lewis base (M-LB), and (d) cooperative metal-Lewis acid (M-LA)

Apart from the Pt/Al complex, Ni/B complex for H_2 activation was also reported in 2012 by Peters and co-workers (Harman & Peters, 2012). The nickel complex with diphosphine borane, $ArB(o\text{-}Ph_2PC_6H_4)_2$ ($^{Ph}DPB^{Ar}$) ligand invoked the role of boron Lewis acid acting cooperatively with Ni for H_2 activation and alkene hydrogenation (Harman & Peters, 2012). Although $Ni(^{Ph}DPB^{Ph})(THF)$ cannot react with H_2 at 60 °C, when using mesityl substituent on the B, $Ni(^{Ph}DPB^{Mes})$ can activate H_2 at room temperature, and further being used to catalyze hydrogenation of styrene (Harman, Lin, & Peters, 2014; Zeng & Sakaki, 2013). In general, Ni is more electropositive than Pt, which can potentially facilitate the oxidative addition processes with a lower energy barrier (Tasker, Standley, & Jamison, 2014).

Herein, we investigated the electronic structures and mechanistic studies of complexes **1Pt(PZ)**, $Pt(PPh_3)(Mes_2PC(=CHPh)Z^tBu_2)$ (Z = B, Al) for H_2 activation with the potential utilization of hydrogenation of ethylene. The corresponding mechanism using **1Ni(PB)** complex was also explored. This computational study will elucidate the key features and provide insight into the reactivity of cooperative metal-Lewis acid complexes.

Methodology

Mechanisms of H_2 activation and ethylene hydrogenation as shown in Figure 2 for **1Pt(PAl)**, **1Pt(PB)** and **1Ni(PB)** were carried out using ωB97XD functional (Chai & Head-Gordon, 2008a, 2008b). All geometry optimizations and frequency calculations were performed in gas phase with singlet spin state geometries using Gaussian 09 program (Frisch, 2016). The basis set 1 (BS1) was used. BS1 includes def2-TZVP for Pt and Ni, (Bergner, Dolg, Küchle, Stoll, & Preuß, 1993; Weigend & Ahlrichs, 2005; Xu & Truhlar, 2011) 6-31++G(d,p) (Hariharan & Pople, 1973; Petersson & Al-Laham, 1991; Petersson et al., 1988) for C and H on the substrates involved in the reactions and for P, Al, B, and O, while 6-31G(d) is for all other atoms. Frequency calculation was carried out to verify that all intermediates contain no imaginary frequency and transition states (TS) have only one imaginary frequency. Solvent correction was performed with SMD continuum solvation model (Marenich, Cramer, & Truhlar, 2009) with dichloromethane solvent parameters on the optimized geometry from the gas phase using ωB97XD functional with basis set 2 (BS2) (Chai & Head-Gordon, 2008a, 2008b). For BS2, def2-TZVP is used for Pt and Ni (Bergner et al., 1993; Weigend & Ahlrichs, 2005; Xu & Truhlar, 2011), and 6-31++G(d,p) for all other atoms (Hariharan & Pople, 1973; Petersson & Al-Laham, 1991; Petersson et al., 1988). Unless otherwise specified, the relative energies mentioned throughout the article are referred to the solvent-corrected relative free energies by ωB97XD/BS2 performed on the gas-phase optimization geometry by ωB97XD/BS1.

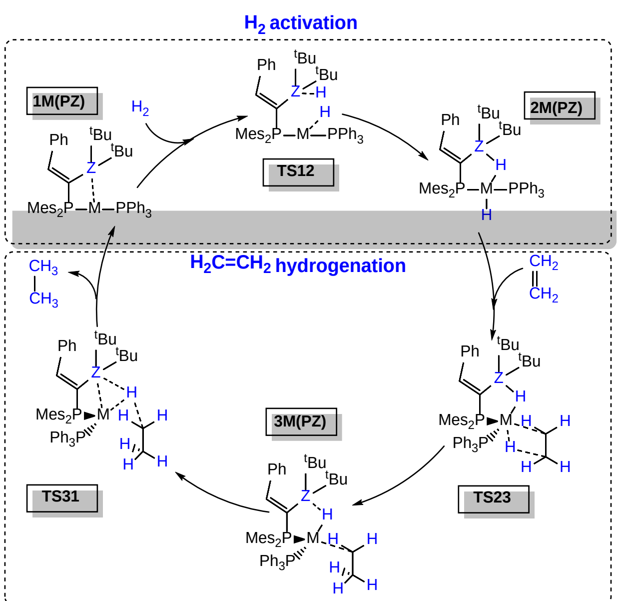

Figure 2. Catalytic cycle of ethylene hydrogenation by cooperative metal-Lewis acid **1M(PZ)** complexes (M = Pt and Ni; Z = B and Al).

Results and Discussion

A. Hydrogen Activation by 1Pt(PAl), 1Pt(PB), and 1Ni(PB)

While $Mes_2PC(=CHPh)Al^tBu_2$ (**PAl**) does not react with H_2,(Appelt et al., 2011) Uhl and co-workers reported that **1Pt(PAl)** activates H_2 at 80.0 °C (Devillard et al., 2016). Our calculation showed that the H_2 activation by **1Pt(PAl)** proceeds via **TS12_PtAl** with a relatively high energy barrier of 31.6 kcal/mol (Figure 3). The trans-dihydride product **2Pt(PAl)** is obtained with slightly exergonic reaction energy of -0.1 kcal/mol.

We further explored the dihydrogen activation by **1Pt(PB)**. With boron in place of aluminum, Pt/B combination shows relatively lower energy barrier of 21.8 kcal/mol for H_2 activation. Correspondingly, the formation of product **2Pt(PB)** is also more favorable thermodynamically with reaction energy of -6.1 kcal/mol.

The interaction between Al and Pt in **1Pt(PAl)** is significant as shown by a rather short distance of 2.624 Å (Figure 4), which leads to rather energy demanding insertion of H_2 to break the stabilizing interaction between metal-Lewis acid. This is in agreement with the X-ray crystal structure reported in the experiment (2.561 Å) (Devillard et al., 2016). In contrast, **1Pt(PB)** shows more elongated bond distance of Pt—B (3.154 Å). With less stabilizing interaction between metal-Lewis acid, the insertion of incoming dihydrogen substrate into Pt/B moiety is more facile.

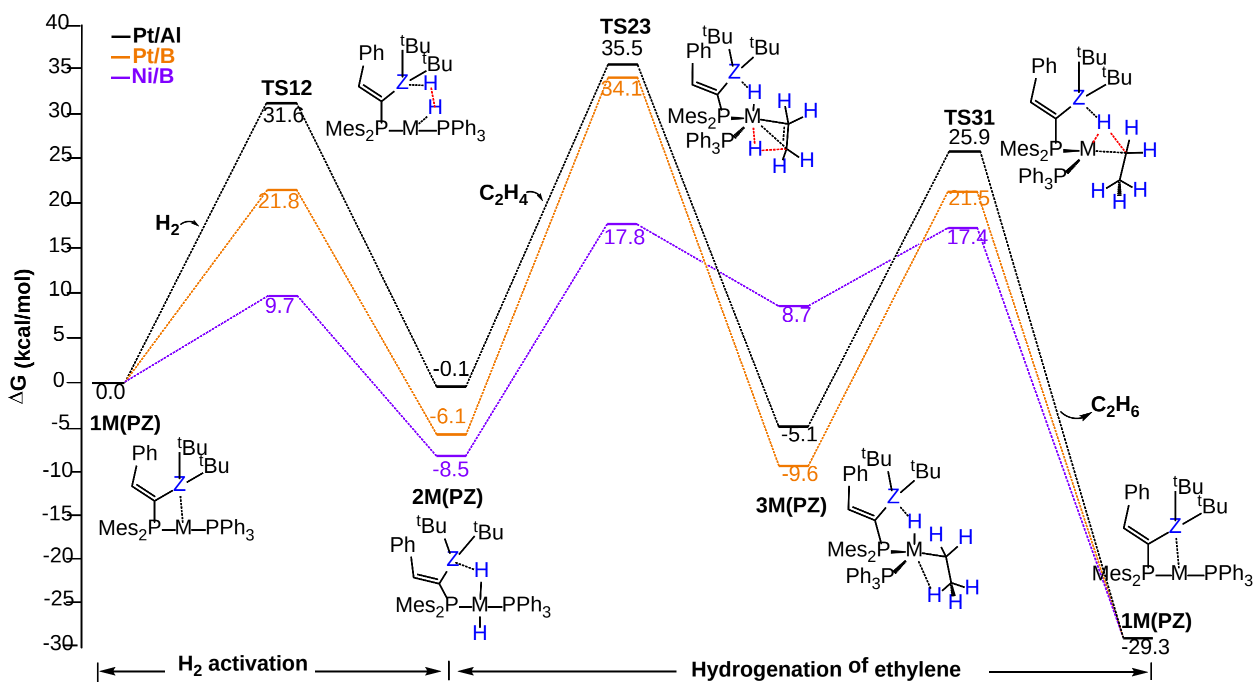

Figure 3. Relative free energy profiles for (i) H_2 activation and (ii) hydrogenation of ethylene by **1Pt(PAl)**, **1Pt(PB)**, and **1Ni(PB)**.

Furthermore, using distortion-interaction analysis of **TS12_MZ**, we are able to gain insights into the energy contributions behind the energy barrier. The energy barrier ($\Delta E^{\ddagger}$) is a sum up of two main contributions: (i) the distortion energy (ΔE_{dist}), which represents the energy for the deformation of reactant/catalyst fragments in the transition state from their free structures, and (ii) the interaction energy (ΔE_{int}), which corresponds to the interfragmental stabilizing interaction between deformed reactant/catalysts (Phipps, Fox, Tautermann, & Skylaris, 2015; Yepes, Jaque, & Fernández, 2018). The interaction energy (ΔE_{int}) of H_2 with **1Pt(PAl)** fragment is considerably more negative (more stabilized) than that with **1Pt(PB)** due to the stronger Lewis acidity of Al than B. In fact, the distortion energy from H_2 fragment (ΔE_{dist_HH}) and **1Pt(PAl)** fragment ($\Delta E_{dist\_M(PZ)}$) of **TS12_PtAl** mainly contribute to the higher destabilization and the higher energy barrier ($\Delta E^{\ddagger}$) for **TS12_PtAl** than that for **TS12_PtB** (Table 1).

Table 1. Distortion-interaction analysis of H_2 activation transition state **TS12_MZ** for **Pt/Al** and **Pt/B** complexes

TS	$\Delta E^{\ddagger}$	$\Delta E_{dist\_M(PZ)}$	ΔE_{dist_HH}	ΔE_{int}
TS12_PtAl	26.0	41.2	92.4	-107.6
TS12_PtB	15.8	28.5	53.3	-66.0

When platinum in **1Pt(PB)** is replaced by nickel, the nickel complex is more reactive towards H_2 than the platinum counterpart. The dihydrogen activation by **1Ni(PB)** is more feasible with the energy barrier of 9.7 kcal/mol (Figure 3) and the formation of product **2Ni(PB)** is also more exergonic with reaction energy of -8.5 kcal/mol.

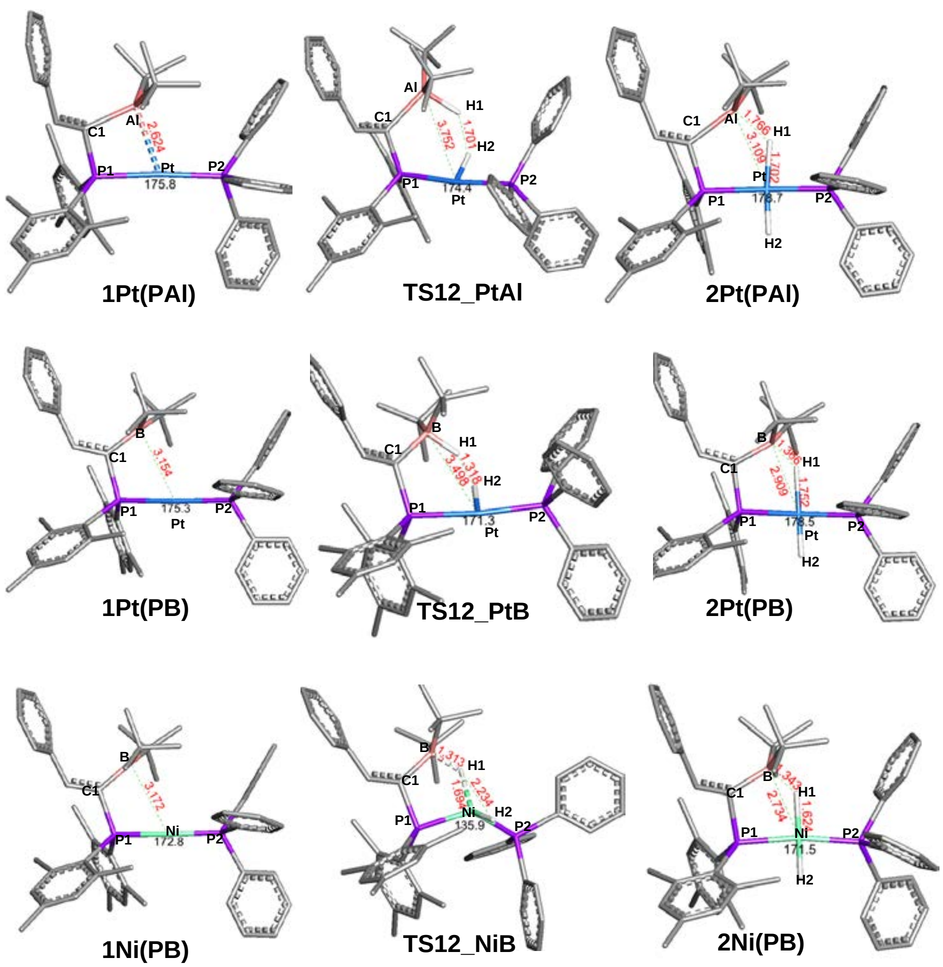

Figure 4. Optimized intermediates and transition states in H_2 activation by **1Pt(PAl)**, **1Pt(PB)**, and **1Ni(PB)**. Selected bond distances are shown in Å. Hydrogen atoms are omitted for clarity except for those from H_2.

The transition state of H_2 activation by Pt complex **TS12_PtB** has the H-H distance of 1.701 Å (Figure 4). The H1 interacts with B while the H2 interacts with Pt. The P1-Pt-P2 remains as linear with the T-shaped geometry. In contrast, the transition state **TS12_NiB** has rather extended H-H distance of 2.234 Å. Notably, the bridging H1 interacts with both B and Ni while the terminal H_2 interacts with only Ni. The P1-Ni-P2 is bent (135.9^o) with the tetrahedral-like geometry. This also can be confirmed from the angle between H1-Ni-H2 and P1-Ni-P2 plane by 85.35^o. While the H_2 is activated by both Pt and B in **TS12_PtB**, it is mainly activated by Ni with an assistance from B in **TS12_NiB**.

Our calculation elucidated that having $Mes_2PC(=CHPh)Z^tBu_2$ (**PZ**) architecture, the **PB** compound can serve as a ligand in complex with Pt or Ni to display a higher reactivity towards H_2 than the **PAl** compound. In addition, **1Ni(PB)** was found to be more reactive towards H_2 than **1Pt(PB)**.

B. Hydrogenation of ethylene by 2Pt(PAl), 2Pt(PB), and 2Ni(PB)

We then explored the addition of ethylene to the H_2-complex to obtain ethane and regeneration of **1M(PZ)**. Firstly, the terminal H2 is transferred from metal in **2M(PZ)** to C3 of ethylene via transition state **TS23_MZ** (Figure 5). Then, the H2—C3 bond is formed in intermediate **3M(PZ)**. Secondly, the bridging H1 is transferred to form the C2—H1 bond via transition state **TS31_MZ**. Noticeably, this second hydrogen transfer is more facile than the first hydrogen transfer (Figure 3). Finally, the ethane is released and **1M(PZ)** is regenerated. Note that several attempts have been made to locate the sigma-complex of ethane to metal as a stable intermediate structure, but they were not successful. The ethane was found to dissociate away from metal center with no energy barrier. That is the desorption step of ethane is facile. Similar circumstance was reported by Sakaki and Zeng in the styrene hydrogenation by nickel borane complex, where the ethylbenzene product can be immediately released (Zeng & Sakaki, 2013).

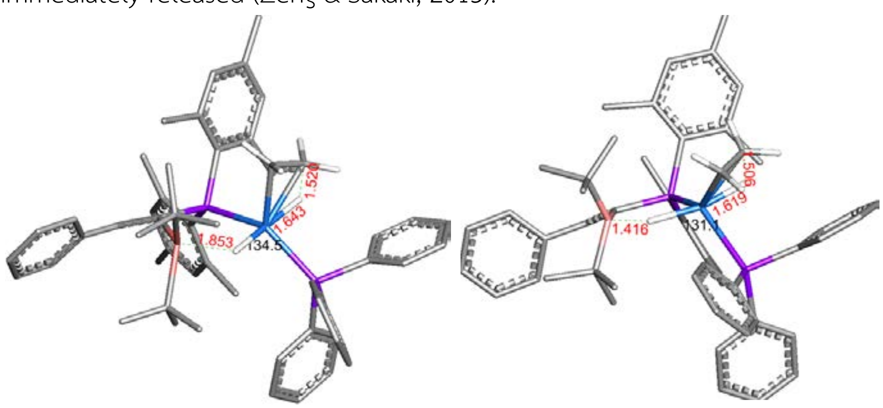

Figure 5. Optimized geometries of the first hydrogen transfer transition state **TS23_PtAl** and **TS23_PtB** in hydrogenation of ethylene. Selected bond distances are shown in Å. Hydrogen atoms are omitted for clarity except for those from H_2.

For the first hydrogen transfer from Pt to C3 of ethylene substrate via **TS23_PtAl**, the energy barrier is relatively high at 35.6 kcal/mol (Figure 3). Upon the binding of ethylene, the P1-Pt-P2 angle is bent from rather linear in **2M(PZ)** to 134.5^o to adopt the trigonal-bipyramidal structure (Figure 5). On the other hand, the hydrogen transfer via **TS23_PtB** proceeds with an even higher energy barrier of 40.2 kcal/mol (Figure 3). The forming H2—C3 distance in **TS23_PtAl** is longer than that in **TS23_PtB** (1.520 Å and 1.506 Å, respectively)

(Figure 5). This indicates that the former is considered as an earlier transition state. Subsequently, the H2—C3 bond is established in intermediate **3Pt(PZ)**. For the second hydrogen transfer from bridging hydrogen H1 to C2, the energy barriers for both **TS31_PtAl** (31.0 kcal/mol) and **TS31_PtB** (31.1 kcal/mol) are similar.

We further investigated **1Ni(PB)** to compare with **1Pt(PB)** in hydrogenation of ethylene. Not only **1Ni(PB)** is more reactive towards H_2 activation, its ethylene hydrogenation by H_2-complex also proceeds with lower energy barriers. The energy barrier for the transfer of terminal hydrogen H2 from Ni to C3 of ethylene via **TS23_NiB** was found more favorable (26.3 kcal/mol) (Figure 3); the H2—C3 distance in **TS23_NiB** is 1.798 Å. Subsequently, H2—C3 bond is formed in intermediate **3Ni(PB)** (1.163 Å) (Figure 6). The **3Ni(PB)** formed can easily proceed to the second hydrogen transfer. The bridging hydrogen H1 is transferred to C2 to form the H1—C2 bond via **TS31_NiB** with the energy barrier of only 8.7 kcal/mol relative to **3Ni(PB)**. The H1—C2 distance is shortened from **3Ni(PB)** to **TS31_NiB** (2.516 Å to 1.712 Å) while the H1—B distance is elongated from 1.394 Å to 2.402 Å. Finally, ethane is eliminated as a product and **1Ni(PB)** is regenerated with the reaction energy of -29.3 kcal/mol (Figure 3).

From the overall mechanism of ethylene hydrogenation by **2M(PZ)**, the rate-determining step is the first hydrogen transfer from terminal H on Ni to form the C-H bond with C of ethylene. The energies required to overcome this step are prohibitively high for **2Pt(PAl)** and **2Pt(PAl)**. Interestingly, this process is feasible for **2Ni(PB)** (26.3 kcal/mol) (Figure 3). Thus, **Ni(PB)** complex can be potentially utilized as a catalyst for hydrogenation of ethylene.

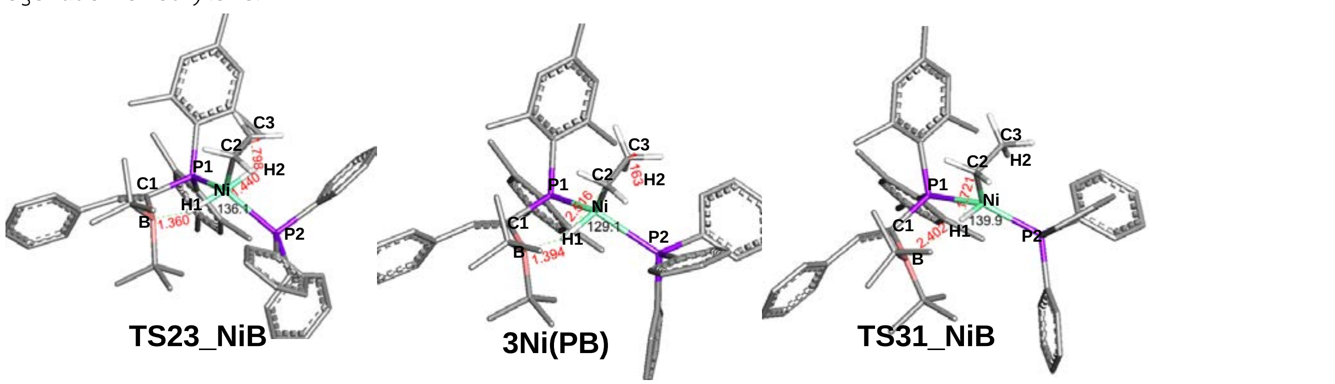

Figure 6. Optimized geometries of all species involved in hydrogenation of ethylene by **2Ni(PB)**. Selected bond distances are shown in Å. Hydrogen atoms are omitted for clarity except for those from H_2.

Conclusions

We investigated the reactivity of cooperative transition metal group 10 complex supported by frustrated Lewis pair $Mes_2PC(=CHPh)Z^tBu_2$ **PZ** (Z = B, Al) compounds towards H_2 activation and ethylene hydrogenation. The use of boron instead of aluminum in ligand architecture in complex **1Pt(PZ)** showed a higher reactivity towards H_2 activation due to the extended Pt—B bond distance compared to Pt—Al. This leads to less energy demanding for insertion of dihydrogen into Pt—B moiety than that into Pt—Al (21.8 kcal/mol and 31.6 kcal/mol, respectively). Furthermore, with more electropositive metal Ni in place of Pt, the energy barrier of dihydrogen activation by **1Ni(PB)** becomes much lower (9.7 kcal/mol). In addition, the reaction energy to form H_2 activation product **2Ni(PB)** is exergonic by -8.5 kcal/mol. This indicates that **1Ni(PB)** has a potential to be used for more feasible reaction towards H_2 activation.

For the reactivity towards ethylene hydrogenation, the first hydrogen transfer from metal to C on ethylene is the rate-determining step of the reaction. Both Pt/Al and Pt/B complexes proceed with relatively high energy barriers (35.6 kcal/mol and 40.2 kcal/mol, respectively). In contrast, the H_2 activation product **2Ni(PB)** can further proceed with a higher reactivity; the first hydrogen transfer rate-determining step has the energy barrier of only 26.3 kcal/mol. From density functional study of metal Lewis acid complexes, the potential application for ethylene hydrogenation could be suggested from the calculated energy required to complete the catalytic cycle. Our calculation suggested that **1Ni(PB)** complex can potentially be served as a catalyst for H_2 activation and ethylene hydrogenation.

Acknowledgments

Financial supports from the Thailand Research Fund (grant no. RSA6280041) and the Center of Excellence for Innovation in Chemistry (PERCH-CIC) are gratefully acknowledged. This research project was supported by the Faculty of Science, Mahidol University.

References

Appelt, C., Westenberg, H., Bertini, F., Ehlers, A. W., Slootweg, J. C., Lammertsma, K., & Uhl, W. (2011). Geminal Phosphorus/Aluminum-Based Frustrated Lewis Pairs: C-H versus C-C Activation and CO_2 Fixation. ***Angewandte Chemie International Edition,*** *50*(17), 3925-3928. doi:10.1002/anie.201006901

Bergner, A., Dolg, M., Küchle, W., Stoll, H., & Preuß, H. (1993). Ab initio energy-adjusted pseudopotentials for elements of groups 13–17. ***Molecular Physics,*** *80*(6), 1431-1441. doi:10.1080/00268979300103121

Chai, J.-D., & Head-Gordon, M. (2008a). Long-range corrected hybrid density functionals with damped atom–atom dispersion corrections. ***Physical Chemistry Chemical Physics,*** *10*(44), 6615-6620. doi:10.1039/B810189B

Chai, J.-D., & Head-Gordon, M. (2008b). Systematic optimization of long-range corrected hybrid density functionals. ***The Journal of Chemical Physics,*** *128*(8), 084106. doi:10.1063/1.2834918

Devillard, M., Declercq, R., Nicolas, E., Ehlers, A. W., Backs, J., Saffon-Merceron, N., . . . Bourissou, D. (2016). A Significant but Constrained Geometry Pt⟶Al Interaction: Fixation of CO_2 and CS_2, Activation of H_2 and $PhCONH_2$. ***Journal of the American Chemical Society,*** *138*(14), 4917-4926. doi:10.1021/jacs.6b01320

Hariharan, P. C., & Pople, J. A. (1973). The influence of polarization functions on molecular orbital hydrogenation energies. ***Theoretica chimica acta,*** *28*(3), 213-222. doi:10.1007/bf00533485

Harman, W. H., Lin, T.-P., & Peters, J. C. (2014). A d10 Ni–(H2) Adduct as an Intermediate in H-H Oxidative Addition across a Ni-B Bond. ***Angewandte Chemie International Edition,*** *53*(4), 1081-1086. doi:10.1002/anie.201308175

Harman, W. H., & Peters, J. C. (2012). Reversible H2 Addition across a Nickel–Borane Unit as a Promising Strategy for Catalysis. ***Journal of the American Chemical Society,*** *134*(11), 5080-5082. doi:10.1021/ja211419t

Holschumacher, D., Bannenberg, T., Hrib, C. G., Jones, P. G., & Tamm, M. (2008). Heterolytic Dihydrogen Activation by a Frustrated Carbene–Borane Lewis Pair. ***Angewandte Chemie International Edition,*** *47*(39), 7428-7432. doi:10.1002/anie.200802705

Karunananda, M. K., & Mankad, N. P. (2017). Cooperative Strategies for Catalytic Hydrogenation of Unsaturated Hydrocarbons. ***ACS Catalysis,*** *7*(9), 6110-6119. doi:10.1021/acscatal.7b02203

Khusnutdinova, J. R., & Milstein, D. (2015). Metal–Ligand Cooperation. *Angewandte Chemie International Edition, 54*(42), 12236-12273. doi:10.1002/anie.201503873

M. J. Frisch, G. W. T., H. B. Schlegel, G. E. Scuseria, M. A. Robb, J. R. Cheeseman, G. Scalmani, V. Barone, G. A. Petersson, H. Nakatsuji, X. Li, M. Caricato, A. Marenich, J. Bloino, B. G. Janesko, R. Gomperts, B. Mennucci, H. P. Hratchian, J. V. Ortiz, A. F. Izmaylov, J. L. Sonnenberg, D. Williams-Young, F. Ding, F. Lipparini, F. Egidi, J. Goings, B. Peng, A. Petrone, T. Henderson, D. Ranasinghe, V. G. Zakrzewski, J. Gao, N. Rega, G. Zheng, W. Liang, M. Hada, M. Ehara, K. Toyota, R. Fukuda, J. Hasegawa, M. Ishida, T. Nakajima, Y. Honda, O. Kitao, H. Nakai, T. Vreven, K. Throssell, J. A. Montgomery, Jr., J. E. Peralta, F. Ogliaro, M. Bearpark, J. J. Heyd, E. Brothers, K. N. Kudin, V. N. Staroverov, T. Keith, R. Kobayashi, J. Normand, K. Raghavachari, A. Rendell, J. C. Burant, S. S. Iyengar, J. Tomasi, M. Cossi, J. M. Millam, M. Klene, C. Adamo, R. Cammi, J. W. Ochterski, R. L. Martin, K. Morokuma, O. Farkas, J. B. Foresman, and D. J. Fox. (2016). **Gaussian 09**, (Revision B.01.) [computer software] Wallingford, CT: Gaussian, Inc.

Marenich, A. V., Cramer, C. J., & Truhlar, D. G. (2009). Universal Solvation Model Based on Solute Electron Density and on a Continuum Model of the Solvent Defined by the Bulk Dielectric Constant and Atomic Surface Tensions. ***The Journal of Physical Chemistry B,*** *113*(18), 6378-6396. doi:10.1021/jp810292n

Morris, R. H. (2015). Exploiting Metal–Ligand Bifunctional Reactions in the Design of Iron Asymmetric Hydrogenation Catalysts. ***Accounts of Chemical Research,*** *48*(5), 1494-1502. doi:10.1021/acs.accounts.5b00045

Noyori, R., Yamakawa, M., & Hashiguchi, S. (2001). Metal–Ligand Bifunctional Catalysis: A Nonclassical Mechanism for Asymmetric Hydrogen Transfer between Alcohols and Carbonyl Compounds. ***The Journal of Organic Chemistry,*** *66*(24), 7931-7944. doi:10.1021/jo010721w

Petersson, G. A., & Al-Laham, M. A. (1991). A complete basis set model chemistry. II. Open-shell systems and the total energies of the first-row atoms. ***The Journal of Chemical Physics,*** *94*(9), 6081-6090. doi:10.1063/1.460447

Petersson, G. A., Bennett, A., Tensfeldt, T. G., Al-Laham, M. A., Shirley, W. A., & Mantzaris, J. (1988). A complete basis set model chemistry. I. The total energies of closed-shell atoms and hydrides of the first-row elements. ***The Journal of Chemical Physics,*** *89*(4), 2193-2218. doi:10.1063/1.455064

Phipps, M. J. S., Fox, T., Tautermann, C. S., & Skylaris, C.-K. (2015). Energy decomposition analysis approaches and their evaluation on prototypical protein–drug interaction patterns. ***Chemical Society Reviews,*** *44*(10), 3177-3211. doi:10.1039/C4CS00375F

Rokob, T. A., & Pápai, I. (2013). Hydrogen Activation by Frustrated Lewis Pairs: Insights from Computational Studies. In G. Erker & D. W. Stephan (Eds.), ***Frustrated Lewis Pairs I: Uncovering and Understanding*** (pp. 157-211). Berlin, Heidelberg: Springer Berlin Heidelberg.

Skara, G., De Vleeschouwer, F., Geerlings, P., De Proft, F., & Pinter, B. (2017). Heterolytic Splitting of Molecular Hydrogen by Frustrated and Classical Lewis Pairs: A Unified Reactivity Concept. ***Scientific Reports,*** *7*(1), 16024. doi:10.1038/s41598-017-16244-1

Spies, P., Erker, G., Kehr, G., Bergander, K., Fröhlich, R., Grimme, S., & Stephan, D. W. (2007). Rapid intramolecular heterolytic dihydrogen activation by a four-membered heterocyclic phosphane–borane adduct. ***Chemical Communications*** (47), 5072-5074. doi:10.1039/B710475H

Tasker, S. Z., Standley, E. A., & Jamison, T. F. (2014). Recent advances in homogeneous nickel catalysis. ***Nature,*** *509*(7500), 299-309. doi:10.1038/nature13274

Tsoureas, N., Kuo, Y.-Y., Haddow, M. F., & Owen, G. R. (2011). Double addition of H_2 to transition metal–borane complexes: a 'hydride shuttle' process between boron and transition metal centres. ***Chemical Communications,*** *47*(1), 484-486. doi:10.1039/C0CC02245D

Weigend, F., & Ahlrichs, R. (2005). Balanced basis sets of split valence, triple zeta valence and quadruple zeta valence quality for H to Rn: Design and assessment of accuracy. ***Physical Chemistry Chemical Physics,*** *7*(18), 3297-3305. doi:10.1039/B508541A

Welch, G. C., Juan, R. R. S., Masuda, J. D., & Stephan, D. W. (2006). Reversible, Metal-Free Hydrogen Activation. ***Science,*** *314*(5802), 1124-1126. doi:10.1126/science.1134230

Welch, G. C., & Stephan, D. W. (2007). Facile Heterolytic Cleavage of Dihydrogen by Phosphines and Boranes. ***Journal of the American Chemical Society,*** *129*(7), 1880-1881. doi:10.1021/ja067961j

Xu, X., & Truhlar, D. G. (2011). Accuracy of Effective Core Potentials and Basis Sets for Density Functional Calculations, Including Relativistic Effects, As Illustrated by Calculations on Arsenic Compounds. ***Journal of Chemical Theory and Computation,*** *7*(9), 2766-2779. doi:10.1021/ct200234r

Yepes, D., Jaque, P., & Fernández, I. (2018). Hydrogenation of Multiple Bonds by Geminal Aminoborane-Based Frustrated Lewis Pairs. ***Chemistry – A European Journal,*** *24*(35), 8833-8840. doi:10.1002/chem.201800864

Zeng, G., & Sakaki, S. (2013). Unexpected Electronic Process of H_2 Activation by a New Nickel Borane Complex: Comparison with the Usual Homolytic and Heterolytic Activations. ***Inorganic Chemistry,*** *52*(6), 2844-2853. doi:10.1021/ic301733r